

## Hydrogen-induced platelets in Ge determined by Raman scattering

M. Hiller, E. V. Lavrov, and J. Weber

*Institute of Applied Physics, TU Dresden, 01062 Dresden, Germany*

(Received 4 August 2004; revised manuscript received 6 October 2004; published 18 January 2005)

Single-crystalline germanium samples exposed to hydrogen plasma are studied by Raman scattering spectroscopy. It is shown that hydrogenation results in two Raman bands at 1980 and 4155  $\text{cm}^{-1}$ , which are assigned to local vibrational modes of Ge–H and  $\text{H}_2$ , respectively. Analysis of polarization sensitive Raman scattering spectra suggests that, similar to the case of silicon, the plasma treatment results in extended planar structures, called platelets, which are aligned along  $\{111\}$  crystallographic planes and whose basic units are Ge–H bonds. The signal at 4155  $\text{cm}^{-1}$  is shown to result from molecular hydrogen trapped within these platelets. Furthermore, the influence of the temperature during plasma treatment is examined and the thermal stability of the platelets is studied by isochronal annealing.

DOI: 10.1103/PhysRevB.71.045208

PACS number(s): 61.72.Ji, 61.72.Nn

### I. INTRODUCTION

High concentrations of hydrogen in Si,<sup>1–5</sup> GaAs,<sup>6</sup> and Ge (Ref. 7) result in the formation of extended planar defects, called platelets. Due to the technological importance most of the studies on platelets have been done on hydrogenated Si.

The platelets generated by exposure of crystalline Si to hydrogen plasma are oriented predominantly along  $\{111\}$  crystallographic planes.<sup>1,5</sup> The analysis of polarization sensitive Raman scattering spectra identified two different platelet structures which coexist in concentrations depending on the sample temperature during hydrogen treatment: At low temperatures, an optical dense structure with a dielectric constant  $\epsilon \approx 14$  without  $\text{H}_2$  is preferred, whereas for temperatures above 100 °C, a structure with  $\epsilon \approx 1$  containing  $\text{H}_2$  molecules dominates.<sup>5</sup> One possible candidate for the optically dense structure is the double layer of  $\text{H}_2^*$  aggregates,  $[\text{H}_2^*]_n^D$ , which has the lowest energy of all proposed models for the  $\{111\}$  platelets according to Zhang and Jackson.<sup>8</sup> On the other hand, Martsinovich *et al.* showed that for lattice dilations below 1.5 Å, the half-stacking fault structure is even more stable.<sup>9</sup> Kim and Chang<sup>10</sup> showed that for further lattice dilations the  $[\text{H}_2^*]_n^D$  configuration transforms into the  $[2\text{Si}-\text{H}+\text{H}_2]_n$  structure, where each Si–Si bond in a  $[111]$  direction is replaced by two Si–H bonds, with  $\text{H}_2$  being trapped between the two hydrogenated Si $\{111\}$  layers, which is also in agreement with Ref. 9. The  $[2\text{Si}-\text{H}+\text{H}_2]_n$  structure is the most plausible candidate for the platelet with  $\epsilon \approx 1$ .

From high resolution transmission electron microscopy (HRTEM) studies on deuterium ion implanted (110) Ge wafers,  $\{111\}$  hydrogen induced platelets with structures similar to the Si case are also known to exist in germanium.<sup>7</sup> In the present study we identify the Raman signals originating from  $\{111\}$  platelets in Ge samples after exposure to hydrogen plasma, analyze the influence of the sample temperature during plasma treatment, and describe the annealing behavior of the defects under consideration.

### II. EXPERIMENTAL

Germanium samples used in this study were *p*-type, Ga-doped, Cz (100) wafers with a resistivity of 25  $\Omega$  cm, purchased from Umicore. The samples were hydrogenated in a remote dc hydrogen plasma for 16 h at temperatures varying from room temperature up to 250 °C. The gas pressure was held at 1.5 mbar. For the isotope substitution experiments hydrogen was replaced by either pure deuterium or a mixture of H:D (50:50). To investigate the thermal stability of the defects under consideration, the samples were annealed under Ar atmosphere for 30 min at varying temperatures.

Raman measurements were performed at room temperature in a pseudobackscattering geometry using the 532 nm line of a Nd:YVO<sub>4</sub> laser for excitation. With the absorption coefficient  $\alpha = 5.57 \times 10^5 \text{ cm}^{-1}$  of Ge for the given wavelength, the estimated probing depth  $1/2\alpha$  is about 9 nm.<sup>11</sup> The incident laser beam made an angle of 40° with the sample normal. The laser power on the sample surface was  $\sim 1$  W. To reduce overheating of the sample, the excitation light was focused on a spot size of about 50  $\mu\text{m} \times 5$  mm using a cylindrical lens. The backscattered light was analyzed using a single grating spectrometer and a liquid nitrogen cooled Si CCD detector array. Spectral resolution was set to 7  $\text{cm}^{-1}$ . Polarization sensitive Raman scattering spectra were calibrated for differences in grating efficiency for light of different polarizations using the reference spectra of a blackbody source.

The scattering geometry is defined with respect to the (100) sample surface: The *x*, *y*, and *z* axes are parallel to the crystallographic orientations  $[100]$ ,  $[010]$  and  $[001]$ , whereas the *y'* and *z'* axes are parallel to  $[011]$  and  $[0\bar{1}1]$ . In the notation  $a(b,c)d$ ,  $a(d)$  refers to the propagation vector of the incident (scattered) light, whereas  $b(c)$  characterizes the polarization vector of the incident (scattered) light. The depolarization ratio,  $\Delta$ , is defined as the ratio of the intensity of the scattered light polarized perpendicular to the incident light, to the intensity of the scattered light polarized parallel to it. In the notation  $\Delta_{[xyz]}$ , the subscript implies that the excitation light is polarized along the  $[xyz]$  axis.

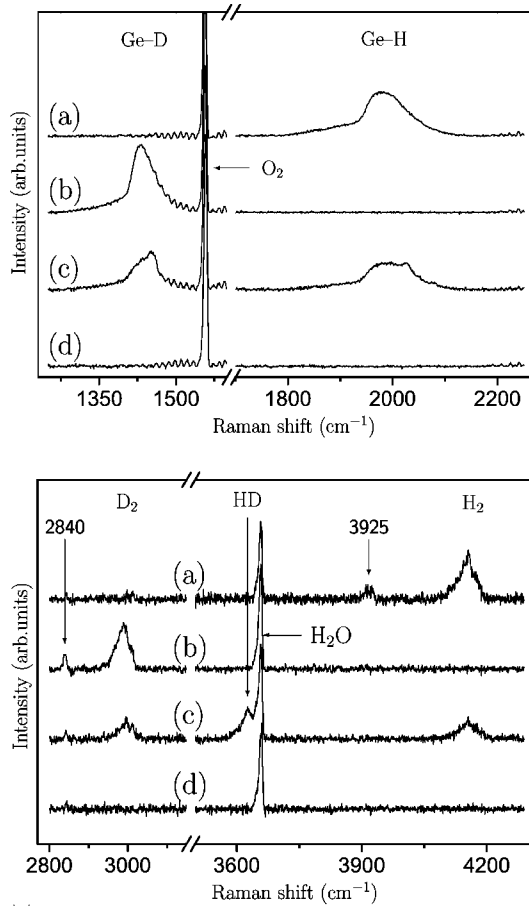


FIG. 1. Room temperature Raman spectra of (100)-Ge after exposure for 16 h at 150 °C to an H- (a), D- (b), and H:D-plasma (50:50) (c), and the reference spectra of a virgin sample (d). Integration time was 20 min for the spectral region 1250–2250  $\text{cm}^{-1}$  and 140 min for the spectral region 2800–4290  $\text{cm}^{-1}$ . Spectra are baseline corrected and offset vertically for clarity.

### III. RESULTS AND DISCUSSION

#### A. Isotope substitution

Figure 1 shows Raman spectra of Ge samples after exposure to hydrogen and/or deuterium plasma at 150 °C for 16 h. The reference spectrum of a virgin sample is given for comparison. The strong Raman line at  $\sim 1556 \text{ cm}^{-1}$  is due to a stretch local vibrational mode (LVM) of atmospheric oxygen,<sup>12</sup> the weaker oscillations around originate from rovibrational transitions of  $\text{O}_2$ . Another Raman line, which is not related to the defects discussed in this work, is located at  $\sim 3657 \text{ cm}^{-1}$  and originates from atmospheric water.<sup>12</sup>

It is seen from the spectra [Fig. 1(a)] that hydrogenation results in two broad Raman bands located at  $\sim 1980$  and  $\sim 4155 \text{ cm}^{-1}$ . The former is reasonably close to the expected frequency of a stretch LVM of Ge–H,<sup>13</sup> the latter one to the frequency of a stretch LVM of free  $\text{H}_2$ .<sup>14</sup> When hydrogen is replaced by deuterium [Fig. 1(b)] the two bands shift downwards in frequency by approximately a factor of  $\sqrt{2}$  to the values of 1430 and 2990  $\text{cm}^{-1}$ , respectively. This proves that these bands originate from stretch LVMs of hydrogen. Fi-

TABLE I. Room temperature frequencies ( $\text{cm}^{-1}$ ) of  $\text{H}_2$  LVMs at the  $T$  sites in semiconductors.

Host	$\text{H}_2$	HD	$\text{D}_2$	Reference
$\text{H}_2$ (free)	4161.1	3632.1	2993.5	14
Si	3601		2622	18
GaAs ( $T_{\text{Ga}}$ )	3912	3429	2827	15,21
GaAs ( $T_{\text{As}}$ )	4043	3541	2920	21
Ge	3925		2840	This work

nally, exposure of a Ge sample to a mixed H:D plasma [Fig. 1(c)] results in the same signals as those shown in Figs. 1(a) and 1(b) plus an additional band at 3625  $\text{cm}^{-1}$  resulting from HD molecules, thus showing that the signal at 4155  $\text{cm}^{-1}$  indeed originates from molecular hydrogen.

So far, the existence of  $\text{H}_2$  has been documented only in Si and GaAs.<sup>15–21</sup> The above findings prove that Ge can host hydrogen molecules as well. An important question concerns the lattice site at which the molecule is trapped. We consider the following possibilities: voids, hydrogen-induced platelets, and interstitial sites.

Table I summarizes the observed frequencies for hydrogen molecules at interstitial tetrahedral ( $T$ ) sites in Si and GaAs. Notice that GaAs is a compound semiconductor and because of this there are two possible interstitial sites for  $\text{H}_2$ : one with Ga closest neighbors ( $T_{\text{Ga}}$ ), the other one with As atoms nearby ( $T_{\text{As}}$ ). It follows from the table that interaction of the molecule with the host atoms results in a considerable drop of the LVM frequency compared to the gas phase value, as is also predicted by theory.<sup>22–24</sup> On the other hand,  $\text{H}_2$  trapped in voids and platelets is much more isolated from the lattice compared to hydrogen at interstitial sites, which leads to its LVM frequency being close to that of the free molecule.<sup>18,21</sup>

Therefore, we conclude that the Raman band at 4155  $\text{cm}^{-1}$  does not originate from  $\text{H}_2$  at interstitial sites of the Ge lattice. Instead, we propose that the molecule is trapped either in voids or in hydrogen-induced platelets. This assignment is supported by the results of polarization sensitive Raman measurements presented in the next section. Moreover, we show that the 4155  $\text{cm}^{-1}$  signal comes from  $\text{H}_2$  trapped within  $\{111\}$  platelets.

Finally, we would like to comment on interstitial  $\text{H}_2$  in Ge. The weak Raman signal at  $\sim 3925 \text{ cm}^{-1}$  seen in Fig. 1(a) could, in principle, be due to interstitial  $\text{H}_2$ . As expected, the line shifts by approximately a factor of  $\sqrt{2}$  to  $\sim 2840 \text{ cm}^{-1}$  when hydrogen is replaced by deuterium [Fig. 1(b)], whereas no Raman signal originating from HD molecules could be observed. It would be very tempting to assign the 3925  $\text{cm}^{-1}$  line to interstitial  $\text{H}_2$  in Ge. Nevertheless, due to experimental difficulties arising from the weakness of the signal, no definite assignment of this Raman line can be made at present.

#### B. Polarization measurements

In this section we want to show that the Ge–H signal at 1980  $\text{cm}^{-1}$  originates from Ge–H bonds aligned along  $\langle 111 \rangle$

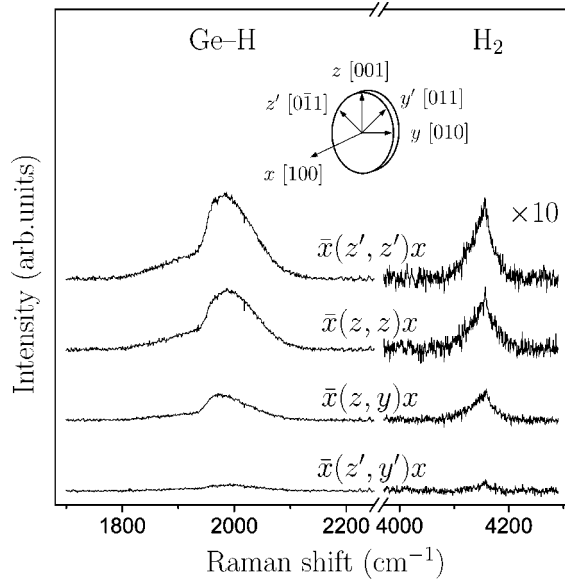


FIG. 2. Scattering geometry and room temperature polarization sensitive Raman spectra measured for a Ge sample after exposure to hydrogen plasma at 125 °C for 16 h. The intensity in the spectral range 4000–4300  $\text{cm}^{-1}$  was scaled up by a factor of 10. Spectra are baseline corrected and offset vertically for clarity.

crystallographic directions, which build up hydrogen-induced  $\{111\}$  platelets. We also show that the  $\text{H}_2$  signal at 4155  $\text{cm}^{-1}$  results from hydrogen trapped within these platelets.

Figure 2 shows polarization sensitive Raman scattering spectra of a Ge sample after exposure to hydrogen plasma. Due to the rather weak Raman intensities, the spectra were obtained only for a sample hydrogenated at 125 °C—the temperature at which the  $\text{H}_2$  signal has the maximum intensity (see Fig. 4). It is seen from the figure that the 1980 and 4155  $\text{cm}^{-1}$  bands have approximately zero intensities for the  $\bar{x}(z', y')x$  geometry, that is for the depolarization ratios we get  $\Delta_{[110]}^i \approx 0$ , where  $i = \text{H}_2$  or Ge–H. We note that the non-zero value of  $\Delta_{[110]}^i$  is caused by a slight misalignment of the sample and nonideality of the polarizer.  $\Delta_{[110]} = 0$  implies that the defects under consideration possess trigonal symmetry and their LVMs are transformed according to the fully symmetric representation  $A_1$ .<sup>25</sup> Because of the vanishing values of  $\Delta_{[110]}^i$ , in the following discussion we consider only  $\Delta_{[100]}^i$ .

Trigonal symmetry is what one would anticipate for the 1980  $\text{cm}^{-1}$  band since one expects the Ge–H bonds to be aligned with the  $\langle 111 \rangle$  axes of the lattice. Interestingly, the  $\text{H}_2$  band at 4155  $\text{cm}^{-1}$  displays the polarization properties of a trigonal defect as well, that is, the hydrogen molecules seem to be aligned along the  $\langle 111 \rangle$  axes of the lattice. This conclusion, however, meets some difficulties. First, the LVM frequency of  $\text{H}_2$  is very close to the free molecule value (see Table I). This implies that the polarization properties of the 4155  $\text{cm}^{-1}$  band should be close to those of free  $\text{H}_2$ , i.e., there should be no preferential direction for the molecule in the crystal. But even if  $\text{H}_2$  were aligned with the  $\langle 111 \rangle$  axes of the lattice, experimentally this would be very difficult to detect. Indeed, from Fig. 2 we obtain  $\Delta_{[100]}^{\text{H}_2} = 0.58 \pm 0.16$ . On

the other hand, from the known Raman tensor of free  $\text{H}_2$  (Ref. 26) one would expect  $\Delta_{[100]}^{\text{H}_2} = 0.022$  for  $\langle 111 \rangle$ -aligned hydrogen molecules. Due to sensitivity restrictions of our experimental setup, this would be hard to distinguish from the expected values  $\Delta_{[110]}^{\text{H}_2} = \Delta_{[100]}^{\text{H}_2} = 0.012$  for  $\text{H}_2$  in randomly oriented voids.

Instead, we propose that our data can be explained if most of the 4155  $\text{cm}^{-1}$  signal originates from  $\text{H}_2$  trapped within  $\{111\}$  platelets, which are known to exist in deuterium ion implanted Ge.<sup>7</sup> We will model these platelets as flat thin dielectric layers oriented along  $\{111\}$  crystallographic planes, which are described by an isotropic, frequency-independent, real dielectric constant  $\epsilon$ . This model has been successfully employed in Ref. 5 to investigate the properties of  $\{111\}$  platelets in Si.

According to the formalism for consideration of dipole radiation in a multilayer geometry proposed by Reed *et al.*,<sup>27</sup> the local electric field in the platelet,  $\mathbf{E}^{\text{loc}}$ , expressed via the  $s$  and  $p$  polarizations of the incident light, can be written as

$$\mathbf{E}^{\text{loc}} = A\mathbf{E}^{\text{in}} = A(\theta_{\text{in}}, \omega_{\text{in}}, \epsilon) \cdot \begin{pmatrix} E_s^{\text{in}} \\ E_p^{\text{in}} \end{pmatrix}, \quad (1)$$

where  $A$  is a  $3 \times 2$  matrix which relates the electric field in the bulk of the sample to the platelet field and depends on (a) the polar angle  $\theta_{\text{in}}$  of the incoming light measured with respect to the platelet normal, (b) the frequency of the incident light  $\omega_{\text{in}}$ , and (c) the dielectric constant  $\epsilon$  of the layer under consideration. Accordingly, the electric field of a radiating dipole  $\mathbf{p}$  situated within this dielectric layer, as seen in the bulk of the sample,  $\mathbf{E}^{\text{sc}}$ , is given by

$$\begin{pmatrix} E_s^{\text{sc}} \\ E_p^{\text{sc}} \end{pmatrix} = \frac{\omega^2}{c^2} A^T(\theta_{\text{sc}}, \omega_{\text{sc}}, \epsilon) \cdot \mathbf{p}, \quad (2)$$

where  $\omega$  is the dipole frequency,  $c$  is the speed of light, and  $A^T$  is the transpose of  $A$ . The indices  $\text{sc}$  refer to the scattered light. Using the Raman tensors  $R^i$  of the considered scatterers, where  $i$  is either Ge–H or  $\text{H}_2$ , the induced polarization  $\mathbf{p}^i$  of an oscillating Raman dipole is given by  $\mathbf{p}^i = R^i \mathbf{E}^{\text{loc}}$ . In the coordinate system where  $z$  is parallel to the bond axis,  $R^i$  is diagonal and  $R_{xx}^i = R_{yy}^i = \delta^i$  and  $R_{zz}^i = 1$ . Taking all this into account, the intensity of the corresponding Raman band,  $I^i$ , is given by

$$I^i \propto \sum_{k \in \langle 111 \rangle} |\mathbf{e}_{\text{sc}} A^T(\theta_{\text{sc}}^k, \omega_{\text{sc}}, \epsilon) R^i A(\theta_{\text{in}}^k, \omega_{\text{in}}, \epsilon) \mathbf{e}_{\text{in}}|^2, \quad (3)$$

where the summation is over all four possible orientations of the  $\{111\}$  platelets in the lattice. Here,  $\mathbf{e}_{\text{in}}$  and  $\mathbf{e}_{\text{sc}}$  are the polarization vectors of the incident and scattered light, respectively. In the case of  $\text{H}_2$ , Eq. (3) is averaged over all possible orientations of the principal axis of  $R^{\text{H}_2}$ , assuming free rotation of the  $\text{H}_2$  molecules within the platelets, whereas for the 1980  $\text{cm}^{-1}$  band we suppose that the Ge–H bonds are aligned along the platelet normal, i.e., along  $\langle 111 \rangle$  crystallographic directions.

$\Delta_{[100]}$  calculated from Eq. (3) for the 1980- and 4155- $\text{cm}^{-1}$  bands as a function of  $\epsilon$  is shown in Fig. 3. The same

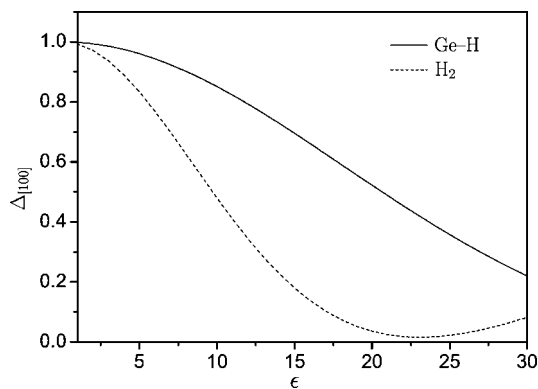


FIG. 3. Calculated depolarization ratios,  $\Delta_{[100]}$ , for the Ge-H and  $H_2$  Raman signals.

calculations yield vanishing values for  $\Delta_{[110]}^{\text{Ge-H}}$  and  $\Delta_{[110]}^{\text{H}_2}$ . Here we assumed that the Raman tensor of  $H_2$  within the platelets is the same as for the free molecule, i.e.,  $\delta^{\text{H}_2} = 0.66$ ,<sup>26</sup> whereas for the 1980- $\text{cm}^{-1}$  band we used  $\delta^{\text{Ge-H}} = 0.25$  obtained from Raman studies on  $\text{GeH}_4$ .<sup>28</sup> Notice that our calculations provide only an estimate for the expected dependency of  $\Delta_{[100]}$  on  $\epsilon$  because the dielectric constant of Ge differs for the incoming and scattered light, so that mean values of  $\epsilon$  for bulk Ge of 22.3 (24.5) were used to obtain  $\Delta_{[100]}^{\text{H}_2}$  ( $\Delta_{[100]}^{\text{Ge-H}}$ ).

From the measurements presented in Fig. 2 we get  $\Delta_{[100]}^{\text{Ge-H}} = 0.39 \pm 0.06$ . Comparison with Fig. 3 shows that this corresponds to  $\epsilon^{\text{Ge-H}} = 24 \pm 2$ , which is about the dielectric constant of bulk Ge for the according wavelength. For the  $H_2$  Raman signal we get  $\Delta_{[100]}^{\text{H}_2} = 0.58 \pm 0.16$ , which corresponds to  $\epsilon^{\text{H}_2} = 8.6 \pm 2.5$ . This is, as one would expect for  $H_2$  gas, well below the dielectric constant of bulk Ge in this spectral region.

### C. Hydrogenation conditions and annealing

Figure 4 shows the integrated intensities of the 1980- and 4155- $\text{cm}^{-1}$  bands as a function of the sample temperature,  $T_s$ , during the hydrogen plasma treatment. It is seen from the figure that the Ge-H related signal is strongest at RT and decreases with increasing  $T_s$ , until it stabilizes for temperatures above 125 °C. Here we want to mention that part of the 1980- $\text{cm}^{-1}$  Raman signal might also originate from Ge-H bonds not involved in the formation of platelets, for example from Ge-H bonds forming voids. The  $H_2$  signal reaches maximum intensity at  $T_s \approx 125$  °C. Thus, the platelet structure seems to depend on the sample temperature during hydrogenation. Since no theoretical studies on platelets in Ge have been published so far, we cannot compare our data with theory and thus conclude how the platelets evolve with the temperature. Another problem comes from the weak intensity of our Raman signals, making it very difficult to perform polarization sensitive Raman studies as a function of  $T_s$ . Even though, based on the similarities between many hydrogen-related defects in Si and Ge reported in the literature,<sup>7,13,29,30</sup> we suggest that possible candidates for the

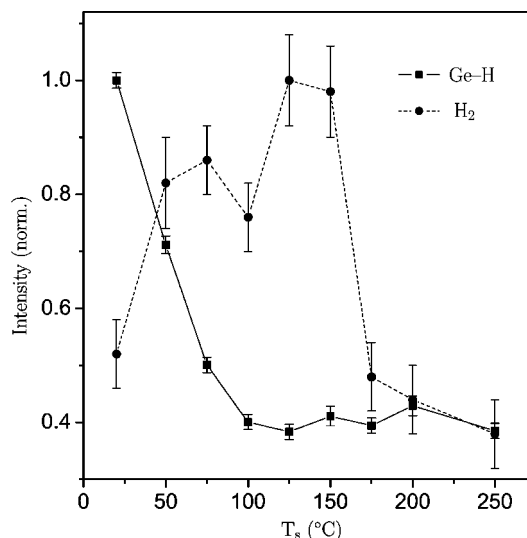


FIG. 4. Dependence of the integrated and normalized intensities of the Raman bands at 1980  $\text{cm}^{-1}$  for Ge-H and 4155  $\text{cm}^{-1}$  for  $H_2$  on the sample temperature  $T_s$  during plasma treatment.

platelet structures in Ge could be  $[\text{H}_2]_n^D$ , the half stacking fault structure, and  $[2\text{Ge-H} + \text{H}_2]_n$ , where the latter holding  $H_2$  could be the one formed at 125 °C.

Finally, the behavior of the Ge-H and  $H_2$  Raman bands under isochronal annealing is shown in Fig. 5. From the figure, the annealing temperatures  $T_a$ , at which the intensities of the corresponding signals are  $1/e$  of the original values, can be estimated as  $T_a^{\text{H}_2} \approx 290$  °C and  $T_a^{\text{Ge-H}} \approx 210$  °C. These temperatures are lower than the corresponding temperatures for the Si case, where the annealing temperature for both Si-H and  $H_2$  is around 400 °C.<sup>18</sup>

## IV. SUMMARY

We presented Raman scattering spectra measured on Ge samples after exposure to hydrogen plasma. Two Raman bands at 1980 and 4155  $\text{cm}^{-1}$  were assigned to stretch LVMs

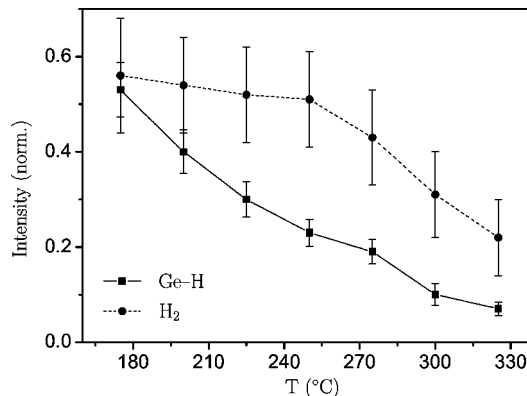


FIG. 5. Annealing of Ge samples hydrogenated at 125 °C. Annealing time was 30 min. All values are normalized to the intensities before the respective annealing step.



of Ge–H and H<sub>2</sub>, respectively. Polarization sensitive Raman measurements suggest that the plasma treatment results in the formation of hydrogen induced platelets oriented along {111} crystallographic planes. The 4155 cm<sup>-1</sup> Raman band is shown to result from molecular hydrogen trapped within these platelets.

### ACKNOWLEDGMENTS

The authors thank B. Hourahine for useful discussions. The work was supported by the Deutsche Forschungsgemeinschaft (WE 1319/14). E.V.L. acknowledges the Russian Foundation for Basic Research (Grant No. 02-02-16030).

- 
- <sup>1</sup>N. M. Johnson, F. A. Ponce, R. A. Street, and R. J. Newmanich, *Phys. Rev. B* **35**, 4166 (1987).
- <sup>2</sup>*Hydrogen in Semiconductors*, edited by J. I. Pankove and N. M. Johnson, *Semiconductors and Semimetals Vol. 34* (Academic, New York, 1991).
- <sup>3</sup>S. J. Pearton, J. W. Corbett, and M. Stavola, *Hydrogen in Crystalline Semiconductors* (Springer-Verlag, Berlin, 1992).
- <sup>4</sup>J. N. Heyman, J. W. Ager III, E. E. Haller, N. M. Johnson, J. Walker, and C. M. Doland, *Phys. Rev. B* **45**, 13 363 (1992).
- <sup>5</sup>E. V. Lavrov and J. Weber, *Phys. Rev. Lett.* **87**, 185502 (2001).
- <sup>6</sup>J. R. Botha, *Proc. Microscop. Soc. A* **27**, 37 (1997).
- <sup>7</sup>S. Muto, S. Takeda, and M. Hirata, *Mater. Sci. Forum* **143–147**, 897 (1994).
- <sup>8</sup>S. B. Zhang and W. B. Jackson, *Phys. Rev. B* **43**, 12 142 (1991).
- <sup>9</sup>N. Martsinovich, M. I. Heggie, and C. P. Ewels, *J. Phys.: Condens. Matter* **15**, 2815 (2003).
- <sup>10</sup>Y.-S. Kim and K. J. Chang, *Phys. Rev. Lett.* **86**, 1773 (2001).
- <sup>11</sup>*CRC Handbook of Chemistry and Physics* (CRC, New York, 2001).
- <sup>12</sup>*American Institute of Physics Handbook* (McGraw-Hill, New York, 1972).
- <sup>13</sup>M. Budde, B. Bech Nielsen, R. Jones, J. Goss, and S. Öberg, *Phys. Rev. B* **54**, 5485 (1996).
- <sup>14</sup>B. P. Stoicheff, *Can. J. Phys.* **35**, 730 (1957).
- <sup>15</sup>J. Vetterhöfer, J. Wagner, and J. Weber, *Phys. Rev. Lett.* **77**, 5409 (1996).
- <sup>16</sup>R. E. Pritchard, M. J. Ashwin, J. H. Tucker, R. C. Newman, E. C. Lightowers, M. J. Binns, S. A. McQuaid, and R. Falster, *Phys. Rev. B* **56**, 13 118 (1997).
- <sup>17</sup>R. E. Pritchard, M. J. Ashwin, J. H. Tucker, and R. C. Newman, *Phys. Rev. B* **57**, R15 048 (1998).
- <sup>18</sup>A. W. R. Leitch, V. Alex, and J. Weber, *Phys. Rev. Lett.* **81**, 421 (1998).
- <sup>19</sup>K. Ishioka, M. Kitajima, S. Tateishi, K. Nakanoya, N. Fukata, T. Mori, K. Murakami, and S. Hishita, *Phys. Rev. B* **60**, 10 852 (1999).
- <sup>20</sup>T. Mori, K. Otsuka, N. Umehara, K. Ishioka, M. Kitajima, S. Hishita, and K. Murakami, *Physica B* **302–303**, 239 (2001).
- <sup>21</sup>E. V. Lavrov and J. Weber, *Physica B* **340–342**, 329 (2003).
- <sup>22</sup>Y. Okamoto, M. Saito, and A. Oshiyama, *Phys. Rev. B* **56**, R10 016 (1997).
- <sup>23</sup>C. G. Van de Walle, *Phys. Rev. Lett.* **80**, 2177 (1998).
- <sup>24</sup>B. Hourahine, R. Jones, S. Öberg, R. C. Newman, P. R. Briddon, and E. Roduner, *Phys. Rev. B* **57**, R12 666 (1998).
- <sup>25</sup>M. Cardona and G. Güntherodt, *Light Scattering in Solids II* (Springer-Verlag, Berlin, 1982).
- <sup>26</sup>C. M. Hartwig and J. Vitko, Jr., *Phys. Rev. B* **18**, 3006 (1978).
- <sup>27</sup>C. E. Reed, J. Giergiel, J. C. Hemminger, and S. Ushioda, *Phys. Rev. B* **36**, 4990 (1987).
- <sup>28</sup>R. Armstrong and R. J. H. Clark, *J. Chem. Soc., Faraday Trans. 2* **72**, 11 (1976).
- <sup>29</sup>M. Budde, B. Bech Nielsen, P. Leary, J. Goss, R. Jones, P. R. Briddon, S. Öberg, and S. J. Breuer, *Phys. Rev. B* **57**, 4397 (1998).
- <sup>30</sup>M. Budde, B. Bech Nielsen, J. C. Keay, and L. C. Feldman, *Physica B* **273–274**, 208 (1999).